MSEC2022-86076

MINIMIZING SHRINKAGE IN MICROSTRUCTURES PRINTED WITH PROJECTION TWO-PHOTON LITHOGRAPHY

Harnjoo Kim Georgia Institute of Technology Atlanta, GA Sourabh K. Saha Georgia Institute of Technology Atlanta, GA

ABSTRACT

Two-photon lithography (TPL) is a photopolymerizationbased additive manufacturing technique capable of fabricating complex 3D structures with submicron features. Projection TPL (P-TPL) is a specific implementation that leverages projectionbased parallelization to increase the rate of printing by three orders of magnitude. However, a practical limitation of P-TPL is the high shrinkage of the printed microstructures that is caused by the relatively low degree of polymerization in the as-printed parts. Unlike traditional stereolithography (SLA) methods and conventional TPL, most of the polymerization in P-TPL occurs through dark reactions while the light source is off, thereby resulting in a lower degree of polymerization. In this study, we empirically investigated the parameters of the P-TPL process that affect shrinkage. We observed that the shrinkage reduces with an increase in the duration of laser exposure and with a reduction of layer spacing. To broaden the design space, we explored a photochemical post-processing technique that involves further curing the printed structures using UV light while submerging them in a solution of a photoinitiator. With this post-processing, we were able to reduce the areal shrinkage from more than 45% to 1% without limiting the geometric design space. This shows that P-TPL can achieve high dimensional accuracy while taking advantage of the high throughput when compared to conventional serial TPL. Furthermore, P-TPL has a higher resolution when compared to the conventional SLA prints at a similar shrinkage rate.

Keywords: additive manufacturing, nanomanufacturing, multi-photon polymerization, print quality,

1. INTRODUCTION

Two photon lithography (TPL) is an additive manufacturing technique that is capable of fabricating arbitrarily-complex three-dimensional (3D) microscale parts with nanoscale features. This unique fabrication method is applicable in a large array of fields such as micro-electro-mechanical systems (MEMS) [1-3], micro-optics [4, 5], microfluidics [6, 7], mechanical/optical metamaterials [8-11], biomimetics [12-14], and biotechnologies [15, 16]. TPL uses laser light to locally cure photo-polymerizable liquid resin into solid features. This mechanism is comparable to the conventional stereolithography (SLA) printing method, but TPL allows fabrication below the diffraction limit, resulting in microscale 3D parts with nanoscale features.

In conventional serial scanning TPL, printing is achieved by focusing high-power near infrared (NIR) femtosecond pulsed laser light into a diffraction-limited spot. This generates focal spot intensities on the order of 1 TW/cm² that are necessary to achieve nonlinear two-photon absorption in the photopolymer material [11]. The nonlinear photo-absorption confines the polymerized region to a fraction of the illuminated region, thereby leading to sub-diffraction printing. Projection TPL (P-TPL) is a high-throughput implementation of TPL wherein more than a million points can be focused at once instead of focusing only a single point [17]. The focal image can be patterned into arbitrary patterns using a digital mask. 3D parts can be printed via a layer-by-layer mechanism.

Although P-TPL increases the rate of printing by three orders of magnitude, the shrinkage of microstructures printed using this technique have not yet been quantified. Shrinkage in printed microstructures results from a combination of shrinkage due to change in phase from liquid to solid and shrinkage due to

structural deformation under the influence of capillary forces generated during development. The shrinkage due to structural deformation can vary widely depending on the mechanical properties of the microstructures [18]. Our goal here is to minimize this structural shrinkage through tuning of the processing conditions.

As the majority of polymerization in P-TPL occurs during the dark [19], the degree of polymerization achieved during P-TPL is expected to be lower than during serial TPL. Previous studies in serial TPL have demonstrated that printing conditions that increase the degree of polymerization lead to improved mechanical properties and are therefore expected to lead to lower shrinkage [20]. However, direct verification of reduction in shrinkage through improved mechanical properties has not been demonstrated in the past. It has been demonstrated that the super critical carbon dioxide (CO₂) drying process [21] and the anchoring method [22] can minimize shrinkage but neither of these techniques achieves this by improving the mechanical properties. Supercritical drying reduces shrinkage by minimizing the forces generated during development whereas the anchoring minimizes shrinkage by disrupting the propagation of strain across the structure. Photochemically curing the printed structure after the printing process has been found to reduce shrinkage by improving the mechanical properties but it has not yet been demonstrated for P-TPL [23].

In this study, we have investigated methods to minimize shrinkage in 3D structures printed using P-TPL through improvements in the mechanical properties. Specifically, we have investigated the effect laser exposure time, layer step size, post-printing UV exposure time, and the concentration of photoinitiator during post processing on shrinkage. Our results can be used to identify design space and post-processing conditions that minimize shrinkage and thereby lead to accurate and uniform printing.

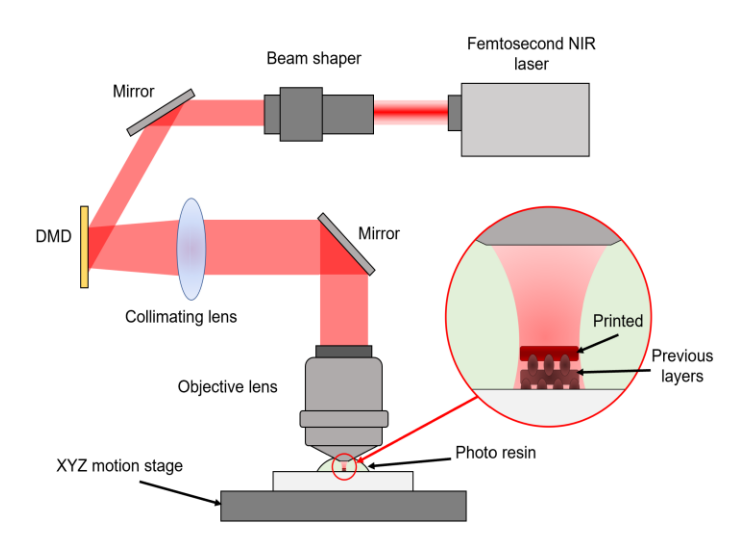


FIGURE 1: Schematic of the P-TPL system.

2. MATERIALS AND METHODS

The P-TPL process is illustrated in Fig. 1. We have used a Ti:Sapphire NIR femtosecond pulsed laser with a center wavelength of 800 nm, pulse repetition rate of 5 kHz, and average power of 1.2 W for processing. Each layer is patterned using a digital mask based on digital micromirror device (DMD). The projection method used in this study requires that the DMD is uniformly illuminated without any intensity variations across the DMD. To achieve this, the Gaussian beam from the laser was modified into a beam with flat-top intensity profile using a refractive beam shaper.

The DMD used in this study consists of 1080 × 1920 microscale mirrors which can be individually turned on or off depending on the corresponding pixel value in the input bitmap image. White pixels in the bitmap image represent "on" states and switching on the mirrors tilts them by +12 degrees and sends the reflected beam towards the collimating lens. Black pixels represent "off" and switching the mirrors off tilts them by -12 degrees. This sends the reflected beam away from the collimating lens. Each mirror is 7.6 µm in width and 7.6 µm in length. The beam emerging from the DMD is therefore patterned by the bitmap image. The patterned beam is then collected by the collimating lens and focused using an objective lens. Here, we have used an oil immersion objective lens with a magnification of 60× and a numerical aperture (NA) of 1.25 NA. The two-lens system demagnifies the bitmap image and projects a demagnified image on the focal plane. The demagnification factor (M_d) can be calculated using Eq. (1) as [17]:

$$M_d = \frac{f_1}{f_2} \tag{1}$$

Here, f_I is the focal length of the objective lens and f_2 is the focal length of the collimating lens.

For our printing process, we have used the dip-in method wherein the lens is directly dipped into the photoresist. This method allows fabrication of 3D structures without height limitations [18] but it requires photoresists of a fixed refractive index (1.52) which is matched to the refractive index of the immersion medium. Here, we have used a custom indexmatched photoresist which consists of a mixture of monmers bisphenol A ethoxylate diacrylate (BPADA) and pentaerythritol triacrylate (PETA). BPADA's refractive index is measured to be 1.542, and PETA's is measured to be 1.49. These two monomers are mixed in a 65:35 ratio to match the refractive index of the objective lens (1.52) in order to reduce the spherical aberration. 4,4'-((1E,1'E)-(2-((2-Ethylhexyl) oxy)-5-methoxy-1,4phenylene)bis(ethene-2,1-diyl))bis(N,N-dibutylaniline) used as a photo initiator and is mixed with the monomer at 0.1% concentration by weight. The single-photon absorption spectrum of the photo initiator is shown in Fig. 2. As the initiator has a high single-photon absorption at half the illumination wavelength (i.e., at 400 nm), it is expected to be suitable for twophoton absorption at 800 nm illumination.

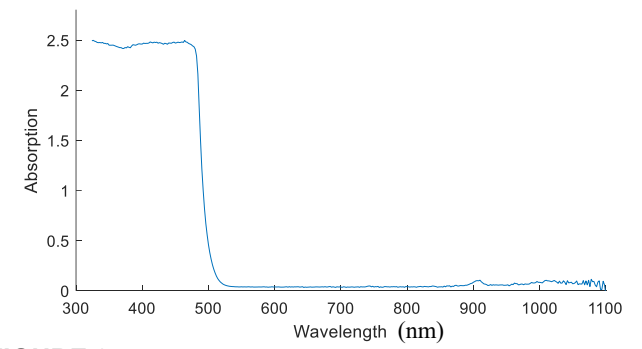


FIGURE 2: Single-photon absorption spectrum of the photoinitiator.

We have quantified the areal shrinkage in dimensions by printing woodpile 3D structures under different conditions. Bitmap images of a series of lines were projected in a staggered configuration as shown in Fig. 3. Staggered formation of the layers aids in optically verifying that each printed layer is distinct from the previous layer without excessive overlap. Shrinkage of the structure was quantified by measuring the area of the topmost layer of the woodpile structure and comparing it against the area of the bottom-most layer. We used optical microscopy to measure the shrunk dimensions of the woodpile structure after the development. Exemplary optical images of the bottom and top layers of the structure are shown in Fig. 4.

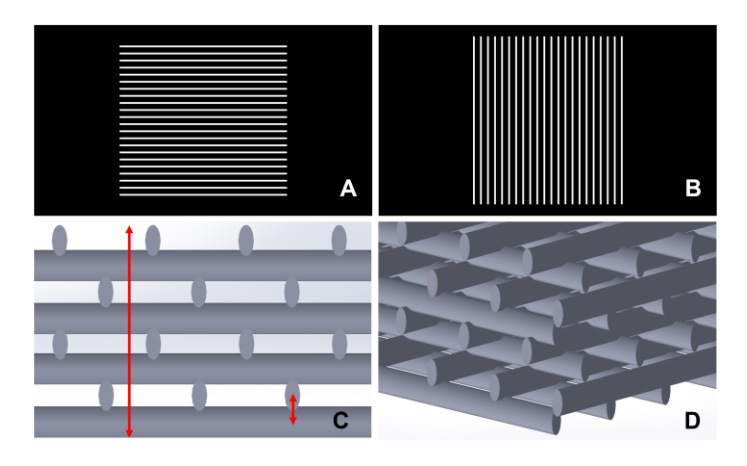


FIGURE 3: (A, B) Bitmap images used for projection of alternate layers. Each image contains a total of 22 lines with each line 10 pixel wide and 950 pixels long. Period of lines is 40 pixels. Vertical lines and horizontal lines are projected alternately in successive layers. (C) Side view of 3D CAD of woodpile structures. Long red arrow indicates the structure height and short red arrow indicates the layer distance (step size). (D) 3D CAD representation of the woodpile structure.

We consider that the bottom-most layer of the woodpile structure does not undergo any structural shrink because it is bonded to the glass substrate during the printing process. The adhesion of the bottom layer with the glass slide prevents the layer's deformation. This was confirmed by comparing the measured dimension to the dimension predicted by Eq. (1). We observed an error of 1.5% in the predicted versus measured

dimensions. It is therefore a reasonable approximation to consider that there is no shrinkage at the bottom layer where it contacts the glass substrate.

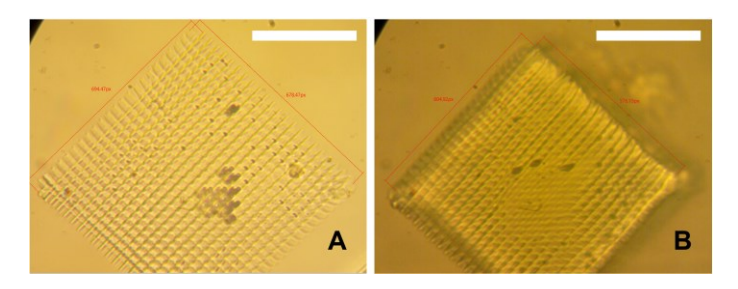


FIGURE 4: Optical microscopy image of (A) Bottom layer of the woodpile structure with dimension of 110 μ m \times 110 μ m and (B) Top surface of the green-state 95 μ m tall woodpile structure printed with 60 ms exposures per layer with 4 μ m layer distances. The measured dimension on this top layer is 95 μ m \times 95 μ m, which translates to an areal shrinkage of 25.4%. Scale bar: 50 μ m.

In this study, we have investigated the effect of varying the exposure time, structure layer distance, and the height of the structure on the amount of shrinkage. We have also investigated the effect of photochemical curing-based post-processing on the shrinkage. The term "green-state" refers to printed structures that have not been further processed with photochemical curing. Green-state structures were developed by dipping the printed microstructures in Propylene glycol monomethyl ether acetate (PGMEA) and isopropyl (IPA) for 10 minutes each, followed by air drying. This development process dissolves the uncured photoresist and washes it away leaving behind the 3D printed microstructure. Microstructures that were photochemically cured underwent the same initial dipping steps but they were further dipped into a solution of a photoinitiator and exposed to flood UV lighting before air drying. We used the 2,2-dimethoxy-2-phenylacetophenone (Irgacure 651) photoinitiator which was dissolved in IPA and generates radicals when exposed to UV light. During the UV curing process, a 4 W 365 nm UV lamp was placed 12 mm away from the printed structure (with a measured intensity of approximately 0.8 mW/cm²). The radicals generated under UV light lead to additional cross-linking within the microstructure. This is expected to increase the degree of polymerization and thereby strengthen the microstructure. In this study, we hypothesize that the control of parameters would either increase or decrease the degree of polymerization of the 3D printed structure, and the greater the degree of polymerization is, the less shrinkage rate would be observed.

3. RESULTS AND DISCUSSION

Before performing the shrinkage experiments, the operating region for the laser exposure time was investigated and it was then varied between 60 ms and 200 ms. We observed that the shrinkage decreases with an increase in laser exposure time. This is most likely because an increase in the exposure time would increase the degree of polymerization which would result in improved mechanical properties. We also observed that the

shrinkage increases with an increase in the distance between the layers. This is likely because of the higher overlap in neighboring layers which occurs when the distances between the print layers are smaller. This higher overlap both stiffens the structure and leads to a higher degree of polymerization. We also note that the photochemically cured prints developed in the Irgacure solution as part of post processing have significantly lower shrinkage than the green-state microstructures (Fig. 5). This is consistent with past observations from literature that photochemical UV curing improves the mechanical property of the printed structures by generating more radicals from the Irgacure which then leads to denser polymer chains [23]. These observations are illustrated in Figs. 5 and 6.

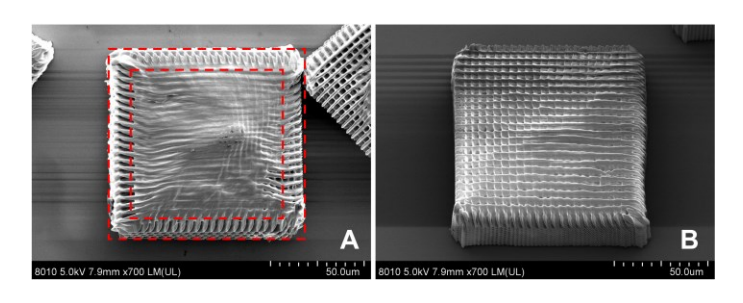


FIGURE 5: Scanning electron micrographs of exemplary 3D woodpile structures. (**A**) Significant shrinkage observed in the structure, which is printed using 100 ms laser exposures per layer, 4 μm layer spacing, and no UV-curing (green-state). (**B**) Little to no shrinkage observed in structure printed using 60 ms, 1 μm layer spacing, UV-curing with 1.0% Irgacure.

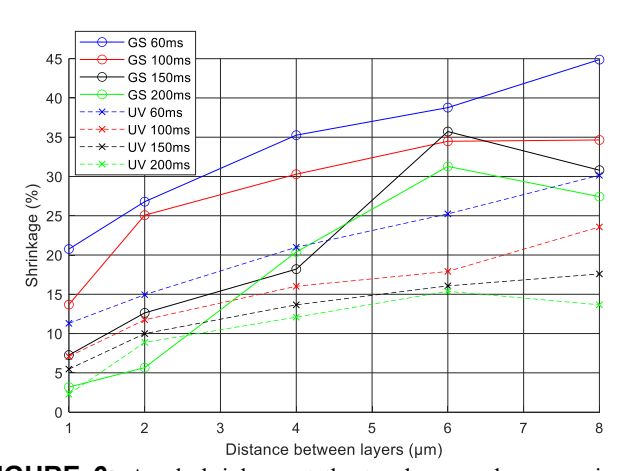


FIGURE 6: Areal shrinkage at the top layer vs layer spacing for green-state/UV cured. Solid lines indicate green-state and dotted lines indicate UV cured state. UV-curing was performed with 1% Irgacure and 10 minutes of UV exposure.

The effect of the duration of UV exposure during photochemical curing on shrinkage in 3D structure is illustrated in Fig. 7. We studied the effect of two different exposures (10 minutes vs 20 minutes of UV exposure) at different laser exposure times of 60 ms and 100 ms. We observed that increased UV exposure led to less shrinkage. Exposing UV for greater

duration would increase the radical generation in the Irgacure, thus producing more polymer chain in the 3D printed structure. This would enhance the mechanical property and reduce shrinkage.

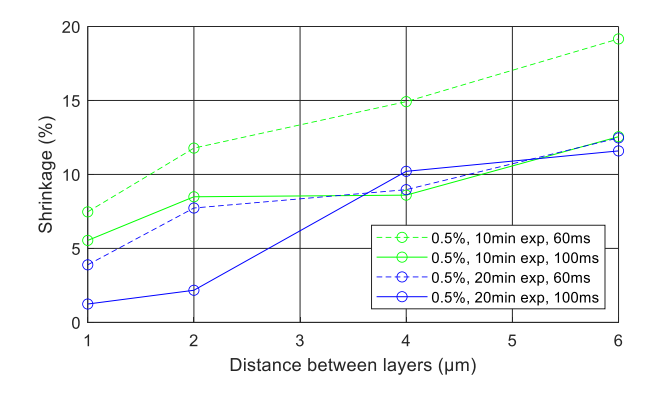


FIGURE 7: Areal shrinkage at the top layer vs layer spacing for different UV exposure time and laser exposure time. All experiments were performed with 0.5% Irgacure.

We also studied the effect of Irgacure concentration on shrinkage, as illustrated in Fig. 8. This experiment was paired with different laser exposure time used in printing and different spacings between the layers of the print. We observed that the shrinkage decreases with an increase in the concentration of Irgacure. This effect is explained by increased radical generation due to increased amount of Irgacure, which would increase the rate of polymer chain formation in the print. This would improve the degree of polymerization and mechanical strength, thereby reducing the shrinkage rate.

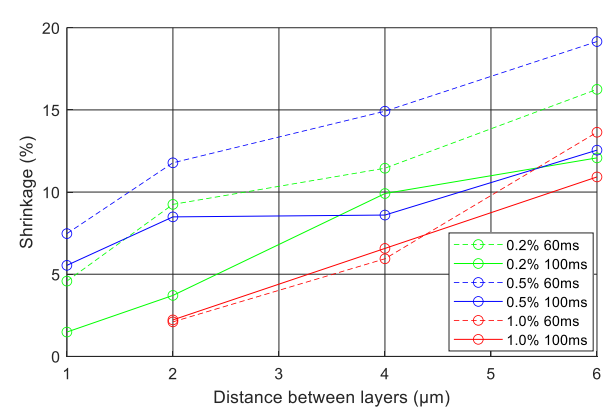


FIGURE 8: Areal shrinkage at the top layer vs layer spacing for different Irgacure photoinitiator concentration and laser exposure time. All experiments were performed with 10 minutes of UV-curing.

It is noteworthy that by increasing the Irgacure concentration during UV-curing to 1%, it is possible to reduce the level of shrinkage at higher layer spacing (2 μm spacing) to the shrinkage at lower layer spacing (1 μm spacing). Thus, the photochemical UV-curing process minimizes shrinkage without compromising the geometric design space of P-TPL. This is highly

advantageous and is in contrast with the capabilities of the anchoring method that relies on specific geometries to minimize shrinkage [22]. In addition, the areal shrinkage can be reduced to as low as 1% suggesting that P-TPL with UV-curing can generate highly accurate structures with low shrinkage-based non-uniformity along the height direction.

Finally, we studied the effect of the height of the printed microstructure on shrinkage. We hypothesized that the taller the structure is, the more shrinkage would be observed because the top-most layer would be further away from the stiff substrate to which the base of the print is rigidly attached. This hypothesis was verified by measuring the area of the top surface and comparing with the area of the bottom surface of the 3D structure as illustrated in Fig. 9. We observe that the shrinkage increases with an increase in the height of the microstructure. Nevertheless, the UV-curing process can be applied to reduce the shrinkage in microstructures of various heights.

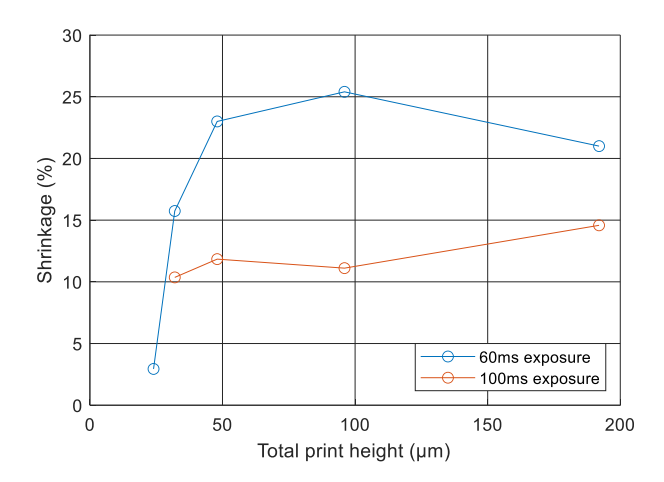


FIGURE 9: Areal shrinkage at the top layer vs height of the 3D microstructure. Both prints are green-states with no UV-curing.

4. CONCLUSION

Shrinkage in 3D printed microstructures deforms the geometry and adversely affects function. Here, we investigated various process parameters to minimize shrinkage in P-TPL. We observed that shrinkage can be reduced by increasing the laser exposure time, concentration of photoinitiator during post-print UV-curing, and the duration of UV exposure. Shrinkage worsens with an increase in the layer spacing and the height of the structure but both these effects can be mitigated by applying the UV-curing post-processing technique. With post-processing, areal shrinkage can be reduced to as low as 1%. This shrinkage rate is comparable to the rate in microstructures printed with conventional serial-scanning TPL and conventional SLA which are known to have higher degree of polymerization than P-TPL. Thus, the shrinkage minimization techniques presented here transform the high-throughput and high-resolution P-TPL process into one capable of achieving high dimensional accuracy. It therefore highlights the potential of P-TPL to be a powerful micro/nanoscale 3D additive manufacturing technique for various applications.

ACKNOWLEDGEMENTS

This work was partly supported by the National Science Foundation CAREER award 2045147. SEM imaging was performed at the Georgia Tech Institute for Electronics and Nanotechnology, a member of the National Nanotechnology Coordinated Infrastructure (NNCI), which is supported by the National Science Foundation (ECCS-2025462).

REFERENCES

- [1] Puce, S., Sciurti, E., Rizzi, F., Spagnolo, B., Qualtieri, A., De Vittorio, M., and Staufer, U., 2019, "3D-microfabrication by two-photon polymerization of an integrated sacrificial stencil mask," Micro and Nano Engineering, 2, pp. 70-75.
- [2] Kurselis, K., Kiyan, R., Bagratashvili, V. N., Popov, V. K., and Chichkov, B. N., 2013, "3D fabrication of all-polymer conductive microstructures by two photon polymerization," Opt. Express, 21(25), pp. 31029-31035.
- [3] Ladner, I., Cullinan, M., and Saha, S., 2019, "Tensile properties of polymer nanowires fabricated via two-photon lithography," RSC Advances, 9, pp. 28808-28813.
- [4] Gissibl, T., Thiele, S., Herkommer, A., and Giessen, H., 2016, "Two-photon direct laser writing of ultracompact multi-lens objectives," Nature Photonics, 10(8), pp. 554-560.
- [5] Steenhusen, S., Stichel, T., Houbertz, R., and Sextl, G., 2010, "Multi-photon polymerization of inorganic-organic hybrid polymers using visible or IR ultra-fast laser pulses for optical or (opto-)electronic devices."
- [6] Sugioka, K., Cheng, Y., and Midorikawa, K., 2005, "Three-dimensional micromachining of glass using femtosecond laser for lab-on-a-chip device manufacture," Applied Physics A, 81(1), pp. 1-10.
- [7] Wu, D., Chen, Q.-D., Niu, L.-G., Wang, J.-N., Wang, J., Wang, R., Xia, H., and Sun, H.-B., 2009, "Femtosecond laser rapid prototyping of nanoshells and suspending components towards microfluidic devices," Lab on a Chip, 9(16), pp. 2391-2394.
- [8] Bückmann, T., Stenger, N., Kadic, M., Kaschke, J., Frölich, A., Kennerknecht, T., Eberl, C., Thiel, M., and Wegener, M., 2012, "Tailored 3D Mechanical Metamaterials Made by Dip-in Direct-Laser-Writing Optical Lithography," Advanced Materials, 24(20), pp. 2710-2714.
- [9] Bauer, J., Meza, L. R., Schaedler, T. A., Schwaiger, R., Zheng, X., and Valdevit, L., 2017, "Nanolattices: An Emerging Class of Mechanical Metamaterials," Advanced Materials, 29(40), pp. n/a-n/a.
- [10] Chaudhary, R. P., Jaiswal, A., Ummethala, G., Hawal, S. R., Saxena, S., and Shukla, S., 2016, "Sub-wavelength Lithography of Complex 2D and 3D Nanostructures without Dyes."
- [11] Valdevit, L., and Bauer, J., 2016, "Chapter 13.1 Fabrication of 3D Micro-Architected/Nano-Architected Materials," Three-Dimensional Microfabrication Using Two-photon Polymerization, T. Baldacchini, ed., William Andrew Publishing, Oxford, pp. 345-373.

- [12] Marino, A., Filippeschi, C., Mattoli, V., Mazzolai, B., and Ciofani, G., 2015, "Biomimicry at the nanoscale: current research and perspectives of two-photon polymerization," Nanoscale, 7(7), pp. 2841-2850.
- [13] Gan, Z., Turner, M. D., and Gu, M., 2016, "Biomimetic gyroid nanostructures exceeding their natural origins," Science advances, 2(5), pp. e1600084-e1600084.
- [14] Kampleitner, C., Changi, K., Felfel, R. M., Scotchford, C. A., Sottile, V., Kluger, R., Hoffmann, O., Grant, D. M., and Epstein, M. M., 2020, "Preclinical biological and physicochemical evaluation of two-photon engineered 3D biomimetic copolymer scaffolds for bone healing," Biomater. Sci., 8(6), pp. 1683-1694.
- [15] Gittard, S. D., Ovsianikov, A., Monteiro-Riviere, N. A., Lusk, J., Morel, P., Minghetti, P., Lenardi, C., Chichkov, B. N., and Narayan, R. J., 2009, "Fabrication of Polymer Microneedles Using a Two-Photon Polymerization and Micromolding Process," Journal of Diabetes Science and Technology, 3(2), pp. 304-311.
- [16] Gittard, S. D., Nguyen, A., Obata, K., Koroleva, A., Narayan, R. J., and Chichkov, B. N., 2011, "Fabrication of microscale medical devices by two-photon polymerization with multiple foci via a spatial light modulator," Biomedical optics express, 2(11), pp. 3167-3178.
- [17] Saha, S., Wang, D., Nguyen, V., Chang, Y., Oakdale, J., and Chen, S.-C., 2019, "Scalable submicrometer additive manufacturing," Science, 366, pp. 105-109.
- [18] Saha, S., Oakdale, J., Cuadra, J., Divin, C., Ye, J., Forien, J.-B., Bayu Aji, L. B., Biener, J., and Smith, W., 2017, "Radiopaque Resists for Two-Photon Lithography To Enable Submicron 3D Imaging of Polymer Parts via X-ray Computed Tomography," ACS Applied Materials & Interfaces, 10.
- [19] Pingali, R., and Saha, S. K., 2021, "Reaction-Diffusion Modeling of Photopolymerization during Femtosecond Projection Two-Photon Lithography," Journal of Manufacturing Science and Engineering, pp. 1-13.
- [20] Jiang, L. J., Zhou, Y. S., Xiong, W., Gao, Y., Huang, X., Jiang, L., Baldacchini, T., Silvain, J.-F., and Lu, Y. F., 2014, "Two-photon polymerization: investigation of chemical and mechanical properties of resins using Raman microspectroscopy," Optics letters, 39(10), pp. 3034-3037.
- [21] Oakdale, J. S., Smith, R. F., Forien, J.-B., Smith, W. L., Ali, S. J., Bayu Aji, L. B., Willey, T. M., Ye, J., van Buuren, A. W., Worthington, M. A., Prisbrey, S. T., Park, H.-S., Amendt, P. A., Baumann, T. F., and Biener, J., 2017, "Direct Laser Writing of Low-Density Interdigitated Foams for Plasma Drive Shaping," Advanced Functional Materials, 27(43), p. 1702425.
- [22] Maruo, S., Hasegawa, T., and Yoshimura, N., 2009, "Single-anchor support and supercritical CO2 drying enable high-precision microfabrication of three-dimensional structures," Opt. Express, 17(23), pp. 20945-20951.
- [23] Oakdale, J. S., Ye, J., Smith, W. L., and Biener, J., 2016, "Post-print UV curing method for improving the mechanical properties of prototypes derived from two-photon lithography," Opt. Express, 24(24), p. 27077.